Molecular Dynamics Simulations of Multicomponent Diffusion. 1. Equilibrium Method

Dean R. Wheeler* and John Newman

Department of Chemical Engineering, University of California, Berkeley, Berkeley, California 94720

Received: May 18, 2004; In Final Form: September 1, 2004

This work demonstrates a general method for simulating multicomponent diffusion in concentrated solutions using molecular dynamics (MD). Although there have been prior reports of MD simulations of diffusion in multicomponent systems, no fully rigorous expressions have been reported for simulating Stefan−Maxwell diffusivities for an arbitrary number of species. The Green−Kubo approach developed here allows for the computation of a full diffusion-coefficient matrix for any number of species. The development is applicable to any solution that can be simulated using MD; nevertheless, our primary interest is in electrochemical applications. To this end, the method is tested by simulations of aqueous KCl and NaCl salt solutions in the concentration range 1−4 *m*. Intermolecular potentials were parametrized for these transport-based simulations. This work is the first to simulate all three independent diffusion coefficients for these solutions. The results are in semiquantitative agreement with experiment and show that Green−Kubo calculations are realizable for concentrated electrolytes and other solutions.

1. Introduction

For many years, adaptations of the Stefan−Maxwell equation have been used successfully to model mass transport in multicomponent concentrated solutions, including electrolytic solutions.[1−5] The chief problem in using these transport equations is obtaining an accurate set of diffusion coefficients. Given that there will never be sufficient experimental data in the literature for all systems of interest, one hopes that theory can bridge the gap. A variety of approaches, including hydrodynamical theory, kinetic theory, absolute-rate theory, and statistical mechanics, have been used on the problem of predicting liquid mass-transport properties.[3,6,7,] Unfortunately, even relatively successful approaches, such as Onsager−Fuoss theory for electrolytes,[8] are limited in application.

Even for the dedicated experimentalist, obtaining the required mass-transport parameters can be daunting. For an isothermal system, the number of independent mass-transport parameters is $n(n-1)/2$ where n is the number of ionic and molecular species. In general, resolving the matrix of diffusion coefficients for concentrated multicomponent solutions requires conducting an orthogonal set of experiments. For instance, for a simple binary electrolyte dissolved in a solvent, there are three independent mass transport parameters. These are typically given as κ (the electrical conductivity), D_s (the salt diffusion coefficient), and t_+^0 (the cation transference number). Values of κ are relatively easy to obtain, and are plentiful in the literature. D_s and t_+^0 are not as easy to obtain, however, and are less frequently reported. The lack of literature data is more severe for electrochemical systems containing greater than three species.

Here we approach the diffusion-prediction problem with statistical mechanics, specifically molecular dynamics (MD). Transport and other properties calculated by MD can be compared directly with experiment to evaluate the veracity of the simulations. Throughout the process, the simulations permit an observable connection between macroscopic material properties and microscopic molecular behavior. Thus, MD shows promise as a tool for predicting and for extending our understanding of transport properties such as diffusion.

It is helpful to differentiate, at this point, a few terms related to diffusion. For our purposes, the terms *self-diffusion* and *tracer diffusion* refer to the same phenomenon: the transport of single molecules due to Brownian motion. We use the terms *collective diffusion*, *bulk diffusion*, and *diffusion* (no designator) interchangeably to refer to transport of species in response to a gradient in activity of that species. *Mutual diffusion* is simply the special case of bulk diffusion in a system with two species. This terminology is in contrast to most of the statistical mechanics literature in which *diffusion* almost always refers to self or tracer diffusion.

The use of MD to simulate collective diffusion has not been extensive. Early work was limited mostly to binary mixtures of Lennard-Jones (LJ) fluids.[9−14] Simulations of penetrant diffusion in membranes have attracted some attention.[15−19] Although systems with three or more components have been simulated,[20,21] we are aware of only one prior study for which a full set of diffusion coefficients is calculated.[22] van de Ven-Lucassen and co-workers purport to develop an MD methodology for simulating ternary Stefan−Maxwell diffusivities;[23,24] however, their mathematical expressions for ternary diffusion are incorrect, as we discuss later. Thus, there is a need for a suitable methodology for calculating collective diffusion coefficients in simulations of an arbitrary number of species.

In this paper (part 1) and the following companion paper (part 2),[25] we demonstrate that MD can be used to calculate all of the relevant mass-transport coefficients for isothermal n-component solutions. This paper will develop an equilibrium or Green−Kubo (GK) expression for calculating diffusivities. Paper 2 will focus on a nonequilibrium method for calculating diffusivities. The theoretical development is applicable to any solution that can be simulated using MD; nevertheless, our primary interest is in electrochemical applications. To this end,

* To whom correspondence should be addressed. Present address: Department of Chemical Engineering, Brigham Young University, Provo, UT 84602. E-mail: dean_wheeler@byu.edu.

10.1021/jp047850b CCC: $27.50
Published on Web 11/02/2004

the method is tested by simulations of aqueous KCl and NaCl salt solutions.

2. Macroscopic Framework

Before embarking on simulation-algorithm development, one must identify what, exactly, are the useful material properties one wishes to simulate. This section sets forth a continuum-level framework relating driving forces to species fluxes, for multicomponent diffusion in concentrated solutions. The material was developed by Newman[1] and is known as concentrated solution theory. Some of the concepts originated with Onsager[2,26,27] and with Hirschfelder et al.[3]

Stefan−Maxwell Equation. The starting point in concentrated solution theory is the assumption of a linear constitutive equation. In this case, it is an adaptation and extension of the Stefan−Maxwell equation, for systems at uniform temperature and pressure

$$c_a \nabla \mu_a = \sum_{b \neq a} K_{ab}(\mathbf{v}_b - \mathbf{v}_a) \tag{1}$$

where the a and b subscripts cover the n species. c is molar concentration, μ is electrochemical potential, K_{ab} is a "friction" coefficient between species a and b, and $\mathbf{v}$ is the species velocity vector. Equation 1 actually describes a set of equations (one for each species a) or a matrix equation. The left side denotes the negative driving force for diffusion of species a and has units of force per volume. The right side expresses a balanced retarding force on a due to interactions with all the other species in solution.

The friction coefficients can be related to diffusivities by

$$K_{ab} = \frac{RTc_a c_b}{c_T \mathscr{D}_{ab}} \tag{2}$$

where R is the universal gas constant, T is the temperature, c_T is the sum of all c_a, and $\mathscr{D}_{ab}$ is a "binary interaction" diffusion coefficient.

For compactness in notation, we represent the driving force (per unit volume) for diffusion as

$$\mathbf{X}_a = -c_a \nabla \mu_a \tag{3}$$

μ is termed the *electrochemical* potential to indicate that composition differences, as well as interactions with an electric potential field, can be used to drive species fluxes. If such are the only thermodynamic driving forces in a system, then

$$\mathbf{X}_a = -\vartheta_a \nabla \Phi - c_a RT \sum_b \Gamma_{ab} \nabla \ln c_b \tag{4}$$

where ϑ_a is the charge density of species a in solution, Φ is the electric potential, and Γ_{ab} is a thermodynamic factor. In turn, $\vartheta_a = Fz_a c_a$, where F is Faraday's constant and z is the species charge number. Incidentally, the original Stefan−Maxwell equation used mole-fraction gradients as driving forces, which is an appropriate choice for its intended use in noncharged gas (ideal solution) mixtures. The notion of driving forces will be expanded further in paper 2.

Comparison of eq 4 to eq 3 gives us a concrete definition for the thermodynamic factors

$$\Gamma_{ab} = \frac{c_b}{RT}\left(\frac{\partial \mu_a}{\partial c_b}\right)_{\Phi,T,P,N_{k\neq b}} \tag{5}$$

In principle, one can calculate the thermodynamic derivative in eq 5 by molecular simulation. Kirkwood and Buff in 1951 related such derivatives to the correlations between fluctuating particle numbers in the grand-canonical ensemble.[28] Because it is not particularly convenient to perform a grand-canonical simulation of a dense liquid, later workers attempted to adapt the method to canonical or microcanonical simulations.[11,12,29] Our initial work along these lines allowed us to generate Γ_{ab} from constant-NPT MD simulations. However, the uncertainties in Γ_{ab} were large enough to make subsequent analysis and comparison with experiment difficult. Although we believe this approach may yet prove fruitful with increased computational effort, we decided to set it aside in order to concentrate our efforts on obtaining the Stefan−Maxwell diffusion coefficients themselves.

Inverted Transport Equation. To form material balances, it is helpful to invert the set of equations (instances of eq 1), so as to express species velocities in terms of driving forces. However, one of the equations in the set is redundant, making only $n - 1$ independent equations. This is due to the fact that $\sum_a \mathbf{X}_a = 0$ by the Gibbs−Duhem relation, applied locally. In the necessary removal of one of the equations, it is advantageous to select a reference velocity at the same time. As Newman recognized, the solvent species velocity, $\mathbf{v}_0$, can be a particularly convenient choice when working with electrolytic solutions.[1] We follow that convention and take the collective velocity of the most preponderant species, the solvent, as the reference. Nevertheless, it is important to note that the choice of reference species (or even of reference velocity) is arbitrary.

With appropriate substitutions, eq 1 can be modified to become

$$-\mathbf{X}_a = \sum_{b \neq 0} M_{ab}(\mathbf{v}_b - \mathbf{v}_0) \tag{6}$$

M_{ab} is defined by

$$M_{ab} = K_{ab} - \delta_{ab} \sum_k K_{ak} \tag{7}$$

where δ_{ab} is the Kronecker delta and k, like a and b, is a species index. The $n - 1$ independent equations corresponding to eq 6 are inverted to become

$$\mathbf{v}_a - \mathbf{v}_0 = \sum_{b \neq 0} L^0_{ab} \mathbf{X}_b \tag{8}$$

where the elements of matrix $\mathbf{L}^0$ are obtained from $\mathbf{L}^0 = -(\mathbf{M}^0)^{-1}$. $\mathbf{M}^0$ results from deleting the column and row corresponding to species 0 from the matrix $\mathbf{M}$ composed of elements M_{ab}. The superscript 0 serves to remind us of the special place for species 0 in the inversion process.

Up to this point, we have given four different representations of transport coefficients: K_{ab}, $\mathscr{D}_{ab}$, M_{ab}, and L^0_{ab}. Each of the four corresponding matrices contains all the necessary mass-transport information for an isothermal system. Moreover, each of the matrices is symmetric, due to Onsager's reciprocal relation.[2] This means that the number of independent transport coefficients for a solution containing n species is $n(n - 1)/2$. The $\mathscr{D}_{ab}$ representation of the mass-transport coefficients is preferred sometimes because it has familiar units of diffusion (m^2/s) and appears to be less concentration dependent than the other representations.

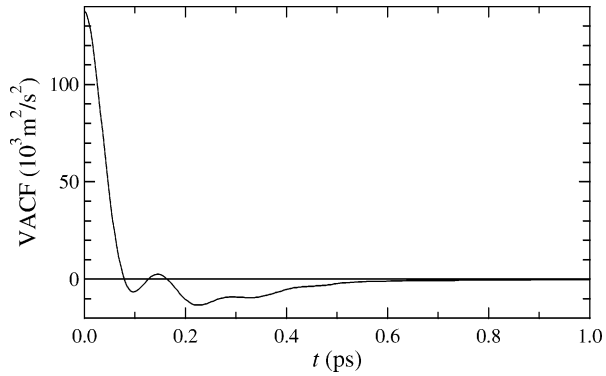

Figure 1. Simulated velocity autocorrelation function (VACF) for liquid water at 298 K.

For electrolytic solutions, the phenomenological eq 8, combined with Ohm's law and the condition of solution electroneutrality, allows us to identify the electrical conductivity as

$$\kappa = \sum_{a\neq 0}\sum_{b\neq 0} L^0_{ab}\vartheta_a\vartheta_b \tag{9}$$

Unlike the values of L^0_{ab}, the value of κ does not depend on the particular choice of reference velocity. As described by Newman, the ion transference numbers and salt diffusion coefficient(s) can be obtained in a similar manner as for κ.[1]

3. Statistical Mechanical Formulation of Diffusion

Green−Kubo Expressions. In formulating a general means of obtaining bulk diffusion coefficients from MD, we draw on the rich history of statistical mechanical work on dynamic and transport phenomena. Expressions to calculate a number of linear transport coefficients in equilibrium ensembles have been known for over 40 years.[30] Today these are known typically as GK expressions or time-correlation formulas. One of the most widely known and used is the GK expression for self-diffusion (or tracer-diffusion in a mixture)

$$D_i^* = \frac{1}{3}\int_0^\infty \mathrm{d}t\, \langle \mathbf{v}_i(t)\cdot\mathbf{v}_i(0)\rangle \tag{10}$$

where angled brackets indicate an ensemble or simulation average and $\mathbf{v}_i(t)$ is the velocity vector of particle i at time t. The integrand is known as a velocity autocorrelation function. Figure 1 shows the results for a realistic model of liquid water at 298 K and 0.1 MPa. As shown, the velocity autocorrelation function has decayed to a small value at 1 ps; integrating the function to at least 1 ps results in a relatively stable value of D_i^*.

The basic principle behind the GK expressions comes from Onsager's famous conjecture known as the regression hypothesis.[26,27] The hypothesis states that the relaxation of an equilibrium system from spontaneous fluctuations due to thermal motion is governed by the same transport coefficients as the relaxation of a nonequilibrium system toward equilibrium, in the limit of linear processes. This means that the natural fluctuations in an equilibrium simulation should contain all the information necessary to calculate linear transport coefficients. These ideas are embodied in the fluctuation−dissipation theorem proved by Callen and Welton and, more generally, in linear response theory.[31,32]

GK expressions have been developed to calculate self-diffusion, mutual diffusion, electrical conductivity, thermal conductivity, shear viscosity, and bulk viscosity.[33,34] In particular, we note a number of works relating to mutual diffusion in binary mixtures of atoms and structured molecules.[10−12,14,16,19,35−41] Stoker and Rowley provide a good review of mutual-diffusion work prior to 1989.[14] Electrical conductivity of ionic solutions has been the subject of several papers.[9,20,30,42,43]

A number of people have recognized that the GK formalism could, in principle, allow the calculation of multicomponent transport coefficients.[23,32,36,44,45] However, we are not aware of any works that establish a correct GK formula for the Stefan-Maxwell transport coefficients given in this work for an arbitrary number of species.

Linear Response Theory. Linear-response theory describes the dynamic behavior of systems close to equilibrium, where external perturbations to the system are small compared to natural thermal fluctuations, as described in a great many papers and monographs.[31,32,44−49] For the work at hand, we use only a part of linear response theory. In particular, we are interested only in calculating diffusion coefficients in the zero-frequency and long-wavelength limits,[50] corresponding to typical experimental transport measurements. Our derivation of a GK expression for Stefan−Maxwell diffusion coefficients is based on the framework and assumptions of linear response theory given by Evans and Morriss.[32,51,52] They show how linear response theory provides a direct connection between a homogeneous nonequilibrium algorithm and the corresponding GK expression to calculate a given transport property. That is, if we can construct an appropriate nonequilibrium algorithm for simulating diffusion, then we can obtain an equilibrium GK formula for diffusion (the reverse technique works as well). Paper 2 goes into greater detail concerning our nonequilibrium algorithm.

What follows is a brief sketch leading to a general expression for a linear response function. That is, we want a function that describes how an arbitrary system property will change under the action of a small external perturbation. Additional details are available from Evans and Morriss.[32,52]

To begin, we introduce the Hamiltonian, $\mathscr{H}_0$, for an equilibrium isothermal N-particle ensemble. $\mathscr{H}_0$ is a conserved quantity, namely the total energy of the relevant degrees of freedom. Next, we impose a small constant external force field on the ensemble beginning at $t = 0$. The new Hamiltonian is

$$\mathscr{H}_1 = \mathscr{H}_0 - \mathscr{R}\mathscr{F} \tag{11}$$

where $\mathscr{R}$ and $\mathscr{F}$ are respectively a generalized position and generalized force, which we leave unspecified at this point. For $t > 0$, the distribution of energy states will evolve under the action of this linear perturbation, according to the Liouville theorem. A numerical thermostat is used to remove heat generated by the $\mathscr{R}\mathscr{F}$ term, so that a steady state in the distribution will result eventually. The expectation value of some system property B at time t can be obtained from the so-called transient time correlation function, derived by Evans and Morriss[52]

$$\langle B(t)\rangle_1 = \langle B(0)\rangle + \frac{1}{k_B T}\int_0^t \mathrm{d}s\, \langle B(s)\dot{\mathscr{R}}(0)\mathscr{F}\rangle_1 \tag{12}$$

The subscript 1 on the angled brackets indicates that averages are taken for the perturbed (nonequilibrium) ensemble. The generalized flux $\dot{\mathscr{R}}$ is the time derivative of $\mathscr{R}$ and is a function of the particle degrees of freedom.

This result may not appear very useful. After all, it is quite easy to calculate $\langle B(t)\rangle$ in a nonequilibrium ensemble without resorting to an integral over a correlation function. The great usefulness of eq 12 comes from the fact that we can analytically

differentiate it to obtain a response function. Proceeding on this thought, we obtain a response function for the arbitrary phase variable B

$$\frac{\partial\langle B(t)\rangle_1}{\partial\mathscr{F}} = \frac{1}{k_B T}\int_0^t \mathrm{d}s\, \langle B(s)\dot{\mathscr{R}}(0)\rangle_1 \tag{13}$$

In the limits $\mathscr{F}\rightarrow 0$ and $t\rightarrow\infty$ this response function measures the steady-state linear response. In this case, the subscript 1 can be removed from the ensemble averages. In other words, the response function becomes a GK-type formula that can be calculated in an equilibrium simulation.

Application to Stefan−Maxwell Framework. With eq 12 in hand, we now approach the problem of multicomponent diffusion. A suitable perturbed Hamiltonian is

$$\mathscr{H}_1 = \mathscr{H}_0 - V\sum_b \mathbf{R}_b\cdot\mathbf{X}_b \tag{14}$$

The species driving forces $\mathbf{X}_b$ are coupled with $\mathbf{R}_b$, the difference between the aggregate centers of mass of species b and species 0

$$\mathbf{R}_b = \frac{1}{N_b}\left(\sum_{i\in b}\mathbf{r}_i\right) - \frac{1}{N_0}\left(\sum_{i\in 0}\mathbf{r}_i\right) \tag{15}$$

The $\mathbf{r}_i$ in eq 15 are "unfolded" coordinates of the molecules in which periodic boundary conditions have not been enforced and only molecules originally occupying the unit cell are included in the sum. Although this is a necessary bookkeeping device for the perturbation term, periodic boundaries are enforced in determining $\mathscr{H}_0$. Moreover, taking the center-of-mass difference between species b and reference species 0 is a subtle but critical step that allows the correct Stefan−Maxwell solution to be generated below.

For clarity, we now introduce the generalized species flux $\mathbf{J}_b$, where $\mathbf{J}_b = \dot{\mathbf{R}}_b = \mathbf{v}_b - \mathbf{v}_0$. The (hypothetical) adiabatic rate of change in $\mathscr{H}_0$ from eq 14 is then

$$\dot{\mathscr{H}}_0^{\mathrm{ad}} = V\sum_b \mathbf{J}_b\cdot\mathbf{X}_b \tag{16}$$

After putting the appropriate substitutions into eq 12, and assuming the $\mathbf{X}_b$ to be constant, we get

$$\langle B(t)\rangle_1 = \langle B(0)\rangle + \frac{V}{k_B T}\int_0^t \mathrm{d}s\, \langle B(s)\sum_b \mathbf{J}_b(0)\cdot\mathbf{X}_b\rangle_1 \tag{17}$$

Again, a subscript 1 indicates that the ensemble corresponding to $\mathscr{H}_1$ is being used to perform the average.

At this stage, we must identify the linear response function that corresponds to the Stefan−Maxwell mass-transport coefficients. The inverted Stefan−Maxwell equation (eq 8) is

$$\mathbf{J}_a = \sum_{b\neq 0} L_{ab}^0\mathbf{X}_b \tag{18}$$

On the other hand, a Taylor series expansion of $\mathbf{J}_a$, truncated to terms linear in $\mathbf{X}_b$, gives

$$\mathbf{J}_a = \sum_{b\neq 0}\left(\frac{\partial\mathbf{J}_a}{\partial\mathbf{X}_b}\right)\mathbf{X}_b \tag{19}$$

Thus, we can immediately identify mass-transport coefficients L_{ab}^0 as

$$L_{ab}^0 = \lim_{t\rightarrow\infty}\lim_{X\rightarrow 0}\frac{\partial\mathbf{J}_a}{\partial\mathbf{X}_b} \tag{20}$$

The infinite-time limit is necessary to ensure a steady-state response, and the zero-field limit is necessary to ensure the linear transport regime.

To obtain L_{ab}^0, we then let $B = \mathbf{J}_a$ in eq 17 and perform the operations indicated by eq 20. This results in the following sequence:

$$\begin{aligned} L_{ab}^0 &= \lim_{t\rightarrow\infty}\lim_{X\rightarrow\infty}\frac{\partial\langle\mathbf{J}_a(t)\rangle_1}{\partial\mathbf{X}_b} \\ &= \lim_{t\rightarrow\infty}\lim_{X\rightarrow\infty}\frac{V}{k_B T}\int_0^t \mathrm{d}s\,\frac{\partial}{\partial\mathbf{X}_b}\langle\mathbf{J}_a(s)\sum_b\mathbf{J}_b(0)\cdot\mathbf{X}_b\rangle_1 \\ &= \lim_{t\rightarrow\infty}\lim_{X\rightarrow\infty}\frac{V}{k_B T}\int_0^t \mathrm{d}s\,\langle\mathbf{J}_a(s)\,\mathbf{J}_b(0)^{\mathrm{T}}\rangle_1 \\ &= \frac{V}{k_B T}\int_0^\infty \mathrm{d}s\,\langle\mathbf{J}_a(s)\,\mathbf{J}_b(0)^{\mathrm{T}}\rangle \end{aligned} \tag{21}$$

The superscript T indicates the transpose. In the final step, taking the limit $X\rightarrow 0$ means that we are no longer operating in a nonequilibrium ensemble. The collective velocity correlation function may be calculated during an equilibrium simulation.

The element L_{ab}^0 above is itself a tensor. From the assumption of isotropic transport, we now let L_{ab}^0 be a scalar quantity, derived from one-third of the trace of the tensor

$$L_{ab}^0 = \frac{V}{3k_B T}\int_0^\infty \mathrm{d}t\,\langle\mathbf{J}_a(t)\cdot\mathbf{J}_b(0)\rangle \tag{22}$$

In a sense, the assumption of isotropic transport allows us to perform an independent "fluctuation experiment" in each coordinate direction and to average the results.

Equation 22 is the GK formula for Stefan−Maxwell diffusivities that we have been seeking. In principle, all independent mass-transport coefficients for an n-component system can be obtained from one equilibrium simulation. Unfortunately, uncertainties in the elements L_{ab}^0 can be high, particularly if either species a or b is in a state of low concentration. The difficulty reduces to the fact that the collective velocity correlation function (the integrand in eq 22) is a property of the entire system and only one value is available at a given time step. The GK formula for tracer diffusion, on the other hand, allows N_a equivalent autocorrelation functions to be collected and averaged at once, for each species a.

Equation 22 satisfies (and is a proof of) Onsager's reciprocal relation (ORR). The principle of microscopic reversibility is an important assumption in any derivation of the reciprocal relation. In this context, microscopic reversibility means that

$$\langle\mathbf{J}_a(t)\cdot\mathbf{J}_b(0)\rangle = \langle\mathbf{J}_a(-t)\cdot\mathbf{J}_b(0)\rangle \tag{23}$$

or that velocity correlation functions are even in time. If we combine this with the principle that correlation functions are invariant to time shifts, we obtain

$$\langle\mathbf{J}_a(t)\cdot\mathbf{J}_b(0)\rangle = \langle\mathbf{J}_a(0)\cdot\mathbf{J}_b(t)\rangle \tag{24}$$

Equation 24 combined with eq 22 is sufficient to demonstrate that $L^0_{ab} = L^0_{ba}$.

In practice, simulation uncertainties will lead to the result that $\mathbf{L}^0$ calculated by our GK formula, eq 22, will not fully obey ORR. To correct this, we make $\mathbf{L}^0$ symmetric by assigning it the value of $(\mathbf{L}^0 + \mathbf{L}^{0T})/2$. The symmetric $\mathbf{L}^0$ is then used to obtain all other bulk-mass-transport properties for the system.

Finally, we note that the GK form for $\mathbf{L}^0$, eq 22, can be converted to an equivalent Einstein form. The result is

$$L^0_{ab} = \frac{V}{6k_BT}\lim_{t\to\infty}\frac{d}{dt}\langle[\mathbf{R}_a(t) - \mathbf{R}_a(0)]\cdot[\mathbf{R}_b(t) - \mathbf{R}_b(0)]\rangle \qquad (25)$$

where, again, $\mathbf{R}_a$ is the vector connecting the center of mass of species a with that of species 0. The conversion of eq 22 to eq 25 requires the use of eq 24; consequently, ORR is automatically satisfied by eq 25.

Prior work has provided GK formulas for multicomponent transport coefficients[32,36,44,45] that have the same basic form as eqs 22 and 25. The present work differs in the peculiar definitions of $\mathbf{J}_a$ and $\mathbf{R}_a$ used in the formulas, and in the mathematical way that the resulting L^0_{ab} is connected to pairwise diffusion coefficients. These distinctions, although subtle, are in fact necessary to calculate transport coefficients rigorously consistent with the Stefan−Maxwell framework described in section 2.

Reduction to Previous Work. An additional test of our GK result in eq 22 is to verify that it reduces to well-known and accepted GK relations for mass-transport properties.

In 1975, Jacucci and McDonald[10] presented a GK formula for a mutual-diffusion coefficient based on a gradient in chemical potential. This formula has been used repeatedly by others to simulate mutual diffusion in binary mixtures of LJ particles and in more structured systems.[11,12,14,16,19,35−41,47] By convention, we label the two species by subscripts 1 and 2, respectively. Jacucci and McDonald's mutual-diffusion coefficient can be expressed in the following form:[11]

$$\mathscr{D}_{12} = \frac{x_1}{3N_2}\left(\frac{N_1m_1+N_2m_2}{m_2}\right)^2\int_0^\infty dt\,\langle\mathbf{v}_1(t)\cdot\mathbf{v}_1(0)\rangle \qquad (26)$$

where m is particle mass of the respective species. x_1 is the mole fraction and $\mathbf{v}_1$ the velocity of species 1.

Now let us compare the above result to the work here. For a two-component system ($a = 1, 2$), with species 1 acting as reference, section 2 tells us

$$L^1_{22} = \frac{c_T\mathscr{D}_{12}}{RTc_1c_2} \qquad (27)$$

Combining this with eq 22 and performing a few cancellations gives

$$\mathscr{D}_{12} = \frac{N_1N_2}{3N}\int_0^\infty dt\langle[\mathbf{v}_2(t) - \mathbf{v}_1(t)]\cdot[\mathbf{v}_2(0) - \mathbf{v}_1(0)]\rangle \qquad (28)$$

Equation 28 is equal to eq 26, which can be seen by substituting into eq 26 a statement of the conservation of linear momentum in the system, $N_1m_1\mathbf{v}_1 + N_2m_2\mathbf{v}_2 = 0$.

In turn, the GK mutual-diffusion formula can be tested by letting $x_1 = 1/N$. This corresponds to the case of a single particle of species 1 diffusing through $N - 1$ particles of species 2. In the limit of large values of N, this procedure leads to the GK formula for tracer diffusion, eq 10. In other words, $\mathscr{D}_{12} \to D_1^*$ in the limit $x_1 \to 0$, which is the result we expect.

There is also a well-known GK expression for electrical conductivity[9,30]

$$\kappa = \frac{1}{3k_BTV}\int_0^\infty\langle\mathbf{i}_c(t)\cdot\mathbf{i}_c(0)\rangle \qquad (29)$$

$\mathbf{i}_c = \sum q_i\mathbf{v}_i$ is the total electrical current in the cell, where q_i is the electrical charge on molecule or ion i. With the substitution of this definition of $\mathbf{i}_c$ and of eq 22 into eq 9, we again arrive at the expected result, eq 29.

It is satisfying that our GK methodology is sufficiently general to describe properly the previously discovered GK relations for mutual diffusion, tracer diffusion, and electrical conductivity. This advantage flows naturally from the use of the Stefan−Maxwell framework as the linear transport law.

Our result, eq 22, does not reduce to a recently proposed GK expression for Stefan−Maxwell diffusivity in a three-component system, given by van de Ven-Lucassen et al.[23,24] Their derivation is not detailed sufficiently for us to identify the source of difficulty. Their final expression for binary Stefan−Maxwell diffusivities in a three-component system is

$$\mathscr{D}_{ab} = \frac{N_b\mathscr{M}}{3m_a}\int_0^\infty\langle\mathbf{v}_b(t)\cdot[\mathbf{v}_b(0) - \mathbf{v}_a(0)]\rangle \qquad (30)$$

$\mathscr{M}$ is the total mass of the system. Equation 30 does not obey the ORR except for certain special cases. In addition, van de Ven-Lucassen et al. offer no explanation as to how their method could be extended to more than three components.

4. Electrolyte Simulations

As a test of the GK formula developed above, we performed simulations for aqueous KCl and NaCl salts. These systems were chosen due to the presence of a substantial body of experimental transport data[53] as well as for their molecular simplicity. We are aware of only one prior work in which a full set of mass-transport coefficients has been calculated for simulations containing three or more species, namely a kinetic Monte Carlo study of ternary diffusion in zeolites by Krishna and Paschek.[22]

Intermolecular Potentials and Algorithm. Because the transport properties we simulate require long computational times, it is desirable to use intermolecular potentials that can be rapidly calculated. The intermolecular potential models used in this work are based on the simple-point-charge (SPC) approach of assigning Coulombic point charges and LJ interaction centers to one or more sites on each molecule. Only pairwise interactions between sites are included in the interaction among different molecules. LJ mixing rules, the treatment of long-range Coulombic potentials via an Ewald sum, and other algorithmic details are discussed in prior work.[54,55]

We used the well-known SPC/E model of water due to Berendsen and co-workers.[56] As a validation of the simulation code, a number of thermodynamic and transport properties of neat water were simulated. The results are compared with experiment in Table 1. Unless otherwise stated, all results given in this paper are for *NPT* simulations, where N is on the order of 3500−4000, $P = 0.1$ MPa, and $T = 298$ K. Simulation uncertainties reported in Table 1, and in the remainder of this work, are standard deviations of the respective means and were obtained by performing block averages during the course of the simulation.[48] Velocity correlation functions were integrated to 10 ps to obtain the mass-transport parameters presented in the next section. The individual simulations were carried out

TABLE 1: Results for SPC/E Water Model Compared to Experimental Data from Refs 57 and 58

property[a]	SPC/E	expt
μ (D)	2.35	2.6−3.0
ρ (g/cm^3)	0.998	0.997
κ_T (GPa^{-1})	0.43 ± 0.03	0.45
η (mPa-s)	0.74 ± 0.05	0.89
ϵ	80 ± 8	78.4
D^* (10^{-9} m^2/s)	2.6 ± 0.1	2.3

[a] μ is dipole moment, ρ is density, κ_T is isothermal compressibility, η is viscosity, ϵ is dielectric constant, and D^* is self-diffusivity.

TABLE 2: Ion Potential Parameters

parameter	K^+	Na^+	Cl^-
q ($\|e^-\|$)	1	1	−1
ϵ/k_B (K)	246	55.3	54.2
σ (nm)	0.285	0.235	0.442

TABLE 3: Ion-Oxygen Distances for the Liquid-Phase First Coordination Shell and Minimum Potential Energies of Ion−Water Pairs[a]

property	K^+	Na^+	Cl^-
$r_{ion\text{-}O}$(nm)	0.276 (0.27−0.29)	0.234 (0.24)	0.324 (0.31−0.34)
ΔE_{pair}(kJ/mol)	−79.5 (−75)	−106.6 (−100)	−50 (−55)

[a] Experimental data in parentheses are from ref 61 and references therein.

for 600 ps, which required about 4 days of computing time on a 1.5 GHz-CPU desktop workstation.

Initially, LJ parameters for the aqueous ions, K^+, Na^+, and Cl^-, were taken from the literature,[43,59,60] but preliminary results showed a large discrepancy between simulated and experimental diffusivities and solution densities. We therefore decided as part of this work to generate new LJ parameters using a semiempirical approach.

Given the use of mixing rules, there are two independent LJ parameters for each of the three ions (one parameter corresponding to the LJ repulsion term and one corresponding to the dispersion term). The dispersion parameters were obtained from estimated dispersion potentials for the real ions, based on their experimental polarizabilities.[61] However, the subsequent simulation results were largely insensitive to the exact choice of dispersion potentials since co-acting Coulombic interactions are so much greater in magnitude. The remaining repulsive parameters were adjusted in an attempt to match (1) experimental solution densities and (2) cation transference numbers at 1 *m* salt concentration. Our attempt to find a suitable ion parameter set was moderately successful, as demonstrated below. Table 2 lists the ion potential parameters.

Simulation Results. Here we present the results, compared to experiment where possible, of our simulations of aqueous KCl and NaCl. For each electrolyte, we performed simulations at three concentrations: 1, 2.5, and 4 *m*.

Table 3 lists two properties that aid us in evaluating whether the actual ion−water potentials have been accurately reproduced by our parameter set. The first property is the most-probable distance between the ion and its first shell of water neighbors in the liquid state. This is obtained from the location of the first peak in the ion−water radial distribution function. We found that this property is largely insensitive to the electrolyte concentration. The simulations are consistent with experiment for this property. The second property is the energy minimum between an isolated ion−water pair, relative to infinite separation. In this case, we do not expect exact agreement with experiment, because our potential parameters are designed for condensed-phase interactions. That is, the potential parameters incorporate, in an average way, the many-body effects that are present in the condensed phase. The approximate agreement of these energies with experiment is fortunate and may indicate that many-body effects are minor when compared to strong pairwise interactions.

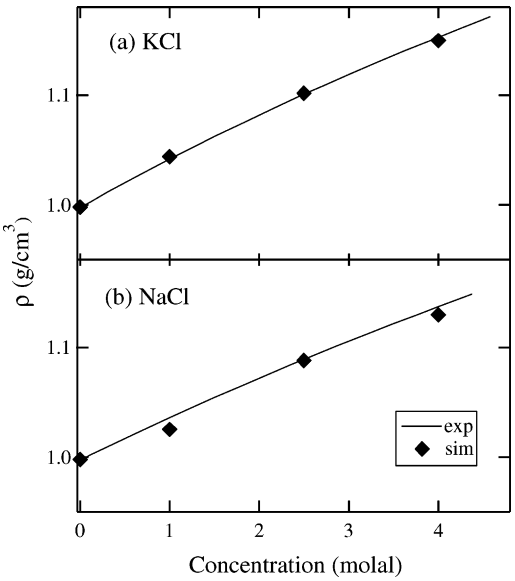

Figure 2. Simulated and experimental solution densities for aqueous KCl and NaCl.

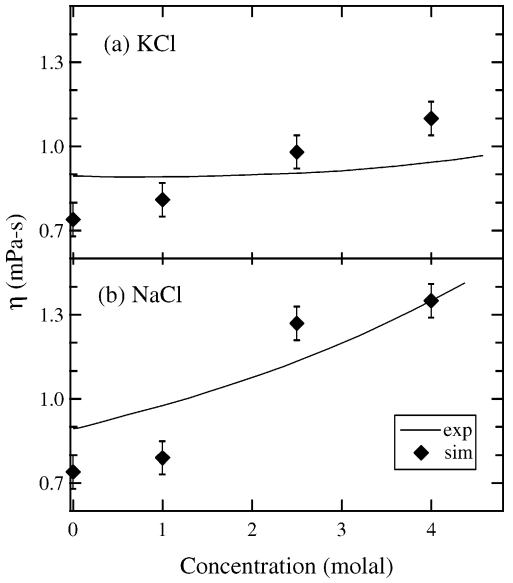

Figure 3. Simulated and experimental solution viscosities for aqueous KCl and NaCl.

Figure 2 gives the simulated electrolytic solution densities as a function of concentration. The experimental data here, and for the transport properties to follow, are based on Chapman's polynomial fits of a compilation of experiments.[53] By design, the simulated densities substantially agree with experiment, as this was one of the considerations used to parametrize the ion potentials. The fact that we could match the density over a range of mixture compositions, by adjusting only pure-component potential parameters, provides evidence that the mixture rules are satisfactory.

The next property to evaluate is shear viscosity, obtained by the GK method.[55,62] As shown in Figure 3, the agreement with experiment is not as satisfying as it is with density, and it appears

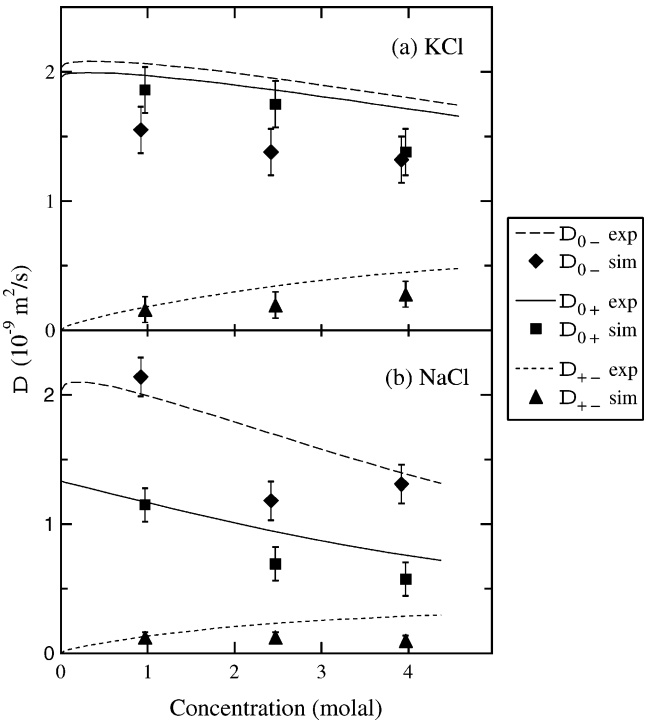

Figure 4. Simulated and experimental Stefan-Maxwell binary diffusivities for aqueous KCl and NaCl. Simulations were performed at 1, 2.5, and 4 *m*; corresponding symbols have been offset horizontally for clarity. Some error bars are smaller in size than the symbols.

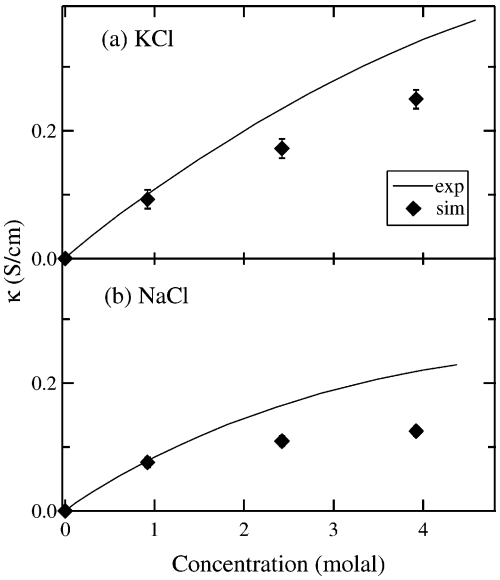

Figure 5. Simulated and experimental conductivities of aqueous KCl and NaCl. Some error bars are smaller in size than the symbols.

that the rate of viscosity increase with concentration is too high. As far as molecular simulations of shear viscosity go, however, agreement with experiment within 20% is uncommonly good. For instance, the SPC/E water model itself underpredicts viscosity by about 18% (see Table 1). Our simulations correctly predict that the viscosity increase upon the addition of KCl to water is less than that for NaCl.

A presentation of the GK-generated Stefan−Maxwell diffusivities is given in Figure 4. The agreement between simulation and experiment is semiquantitatively correct. One difficulty that we were not able to correct was that Cl^- exhibited simulated diffusivities less than than those for K^+, contrary to experiment (Our ion potential models are not the only ones to suffer from this difficulty[43]). Also, $\mathscr{D}_{+-}$ for NaCl shows an incorrect trend with concentration, even when allowing for the error estimates. Nevertheless, these results are quite satisfying when one considers the relative simplicity of the potential models and that the calculations were performed for only a few thousand molecules over a few hundred picoseconds.

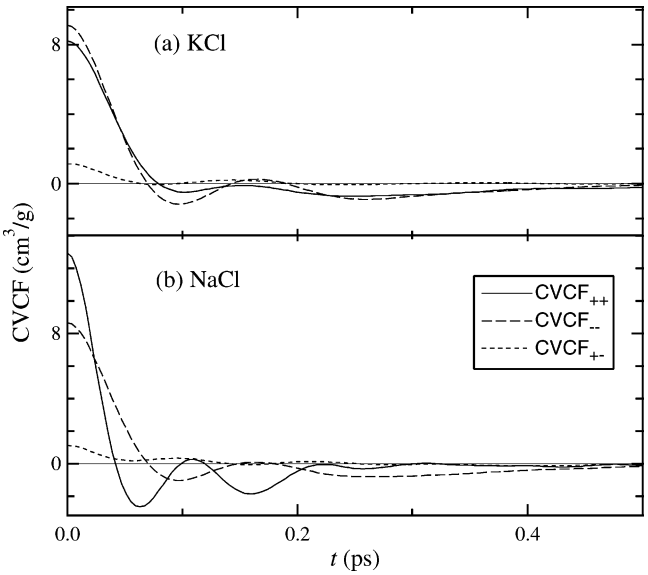

Figure 6. Collective velocity correlation functions (CVCF) for 4 *m* KCl and NaCl.

Figure 5 gives the mass-transport data in another form, namely conductivity. As shown in Figures 4 and 5, the simulations systematically underpredict the mass-transport coefficients. This is most manifest in those properties that are particularly sensitive to ion−ion frictional resistance, namely κ and $\mathscr{D}_{+-}$. It is likely that the ion−ion interactions are too strong, either directly or as a consequence of too weak ion−water interactions. There is a delicate balance of force interactions in the real fluid that is partially, but not fully, reproduced by the simulations. At the higher concentrations, our models' underprediction of diffusion is consistent with its overprediction of viscosity, according to the Stokes−Einstein model of diffusion.

Additional information on bulk ion motion can be gleaned from the collective velocity correlation functions (CVCF) themselves

$$\mathrm{CVCF}_{ab}(t) = \frac{V}{3k_{\mathrm{B}}T}\langle[\mathbf{v}_a(t) - \mathbf{v}_0(t)]\cdot[\mathbf{v}_b(0) - \mathbf{v}_0(0)]\rangle \qquad (31)$$

The time integration of CVCF_{ab} yields eq 22, the GK expression for L^0_{ab}. In the limit of infinite dilution of solute species *a*, CVCF_{aa} becomes proportional to the velocity autocorrelation function (VACF), $\langle \mathbf{v}_i(t)\cdot\mathbf{v}_i(0)\rangle$, the single-particle property used in the GK expression for tracer diffusion, eq 10.

Figure 6 shows the CVCF_{ab} for 4 *m* KCl and NaCl. (At other concentrations, these functions have substantially the same shape.) The shapes of the CVCF_{++} and CVCF_{--} functions can be evaluated on the same footing as the corresponding single-particle VACFs. We see "backscattering" dips at 0.1 and 0.25 ps for the CVCF_{++} for K^+ and the CVCF_{--} for Cl^-. These, not coincidently, are the same backscattering features exhibited by pure water, as given by the VACF of Figure 1, and illustrate the intimate connection between an ion's diffusion and the behavior of the surrounding solvent. The CVCF_{++} for Na^+, however, has a second higher-frequency signal superimposed on its backscattering region. This is due to the Na^+ rattling

within its cage of neighbors, motions that do not contribute significantly to long-time displacement, that is, macroscopic diffusion.

A well-received analysis of the single-particle diffusion of ions at infinite dilution is given by Impey et al.[63] In that report, the authors illustrate how there is a fundamental difference between the tracer diffusion of Na^+ on one hand and K^+ and Cl^- on the other hand. Although all three ions have reasonably similar coordination numbers (numbers of waters in the first solvation shell), in the case of Na^+, the waters are more tightly bound to the ion. The residence time, a time constant relating to how long a water molecule spends in the ion's coordination sphere, is about twice as large for Na^+ as it is for K^+ and Cl^-. On the time scale of ion diffusion, Na^+ stays with its first shell of neighbors, whereas K^+ and Cl^- are more likely to shed or exchange coordinated waters.

The curves for $CVCF_{+-}$ in Figure 6 for both KCl and NaCl are nearly identical. This function measures the correlation between bulk motion of the cation with that of the anion. There is no single-particle analogue to this property. The apparent lack of a negative region means there is no backscattering effect; on average, equilibrium bulk counterion motions reinforce rather than oppose each other. The fact that the $CVCF_{+-}$ curves decay to zero on a reasonably short time scale teaches us that ion relaxation is not a long-time phenomenon at higher electrolyte concentrations.

There is some disagreement in the literature as to whether collective velocity correlation functions decay to zero faster than corresponding single-particle functions.[14,64] Analysis is made more difficult by the fact that the collective-diffusion data invariably have more noise than the self-diffusion data. Our simulation results are not able to settle this question. We carried out the GK time integrations to 10 ps, well beyond the time when a clearly defined signal could be observed through the noise. Integrations of correlation functions to long times do not necessarily improve the reliability of the result, due to the accumulation of noise that can exceed the accumulation of the signal of interest. In fact, integration of the noise in the correlation function is like performing a random walk, in which the variance and hence uncertainty of the result grows linearly with time.

5. Conclusion

In this paper, we have developed a new GK expression to calculate all independent mass-transport parameters in a mixture of an arbitrary number of species. The simulations show that the method can be implemented for a realistic model of an electrolyte.

It has been argued by Barthel and others that one cannot obtain diffusion of ions in solution using GK expressions and molecular dynamics. This is because of the large characteristic time (claimed to be about 1 ns) required for relaxation of the ionic atmosphere about each ion, leading to a large long-time tail in ion GK formulas.[65,66] However, we do not observe this problem in our simulations. Perhaps the resolution of this discrepancy is the fact that we are simulating in the concentration range of 1−4 *m*. As noted by Pitzer and Simonson, the relaxation effect is a manifestation of long-range electrostatic interactions.[67,68] However, at high ionic concentrations, the long-range electrostatic interactions are effectively screened, and short-range electrostatic interactions take on greater importance. This phenomenon is qualitatively described by Debye−Hückel theory. For instance, the Debye lengths for our simulations range from 0.15 to 0.3 nm (compared to cubic cell lengths of around 5 nm), meaning that short-range interactions play a large role in the distribution of ions. The agreement of our equilibrium and nonequilibrium simulation results, discussed in paper 2, provides further evidence that it is possible to use GK expressions and molecular dynamics to simulate ion diffusion in concentrated solutions.

In practice, the use of MD to calculate bulk mass transport is limited to concentrated solutions. In addition to the possible relaxation-time scale problem mentioned above, there is the difficulty in having a sufficient number of ions on which to collect statistics. Put another way, with decreasing electrolyte concentration, it becomes increasingly expensive to calculate the growing number of solvent interactions for a fixed number of ions. In the future, the use of the generalized Langevin framework may allow a bridge between concentrated solutions simulated by MD and dilute solutions treated by analytic theory. In the generalized Langevin framework, the solvent degrees of freedom are treated approximately, and only the solute degrees of freedom are retained explicitly. This allows significantly smaller solute concentrations and longer times to be simulated, at the cost of accuracy. However, the loss of accuracy can be managed by ensuring that the Langevin simulations match the analytic theory and MD simulations at the low and high ends, respectively, of the concentration range.

A separate issue is the agreement between our simulations and experiment. For aqueous KCl and NaCl, the agreement is reasonably good, by molecular-simulation standards, but needs to be improved before the simulations can be considered quantitatively correct. The crux of the issue is the accuracy of the potential models. In order for the models to succeed at high concentrations, nearest neighbor interactions must be faithfully reproduced. It may be that the addition of explicit polarizability combined with a more accurate treatment of short-range interactions will improve the models. This has been tried many times before: aqueous solutions have been the subject of a great deal of simulation work. It is tempting in the face of so much prior work to conclude that simple intermolecular potential models will not be able to generate quantitatively accurate transport properties. Nevertheless, our success thus far heartens us to the prospect.

Acknowledgment. This work was supported by a National Science Foundation graduate fellowship and by the Assistant Secretary for Energy Efficiency and Renewable Energy, Office of FreedomCAR and Vehicle Technologies of the U.S. Department of Energy under Contract No. DE-AC03-76SF00098.

References and Notes

(1) Newman, J. *Electrochemical Systems*, 2nd ed.; Prentice Hall, Englewood Cliffs, NJ, 1991.
(2) Onsager, L. *Ann. N.Y. Acad. Sci.* **1945**, *46*, 241−265.
(3) Hirschfelder, J.; Curtiss, C.; Bird, R. *Molecular Theory of Gases and Liquids*; Wiley: New York, 1954.
(4) Wendt, R. *J. Phys. Chem.* **1965**, *69*, 1227.
(5) Miller, D. *J. Phys. Chem.* **1966**, *71*, 616.
(6) Reid, R.; Prausnitz, J.; Poling, B. *The Properties of Gases and Liquids*, 4th ed.; McGraw-Hill: New York, 1987.
(7) Erdey-Gruz, T. *Transport Phenomena in Aqueous Solutions*; Akademiai Kiado: Budapest, 1974.
(8) Onsager, L.; Fuoss, R. *J. Phys. Chem.* **1932**, *36*, 2689−2778.
(9) Hansen, J.-P.; McDonald, I. R. *J. Phys. C* **1974**, *7*, L384-L386.
(10) Jacucci, G.; McDonald, I. *Physica A* **1975**, *80*, 607−625.
(11) Jolly, D. L.; Bearman, R. J. *Mol. Phys.* **1980**, *41* (1), 137−147.
(12) Schoen, M.; Hoheisel, C. *Mol. Phys.* **1984**, *52* (1), 33−56.
(13) Morriss, G. P.; Evans, D. J. *Mol. Phys.* **1985**, *54*, 629.
(14) Stoker, J.; Rowley, R. L. *J. Chem. Phys.* **91**, *91* (6), 3670−3676.
(15) Müller-Plathe, F.; Rogers, S. C.; van Gunsteren, W. F. *J. Chem. Phys.* **1993**, *98* (12), 9895−9904.
(16) MacElroy, J. *J. Chem. Phys.* **1994**, *101* (6), 5274.

(17) Sunderrajan, S.; Hall, C. K.; Freeman, B. D. *J. Chem. Phys.* **1997**, *107* (24), 10714−10722.
(18) Thompson, A. P.; Heffelfinger, G. S. *J. Chem. Phys.* **1999**, *110* (22), 10693−10706.
(19) Arya, G.; Chang, H.-C.; Maginn, E. J. *J. Chem. Phys.* **2001**, *115* (17), 8112−8124.
(20) Payne, V. A.; hua Xu, J.; Forsyth, M.; Ratner, M. A.; Shriver, D. F.; de Leeuw, S. W. *Electrochim. Acta* **1995**, *40* (13−14), 2087−2091.
(21) Soetons, J.-C.; Millot, C.; Maigret, B. *J. Phys. Chem. A* **1998**, *102* (7), 1055−1061.
(22) Krishna, R.; Paschek, D. *Chem. Eng. J.* **2002**, *87*, 1−9.
(23) van de Ven-Lucassen, I. M.; Vlugt, T. J.; van der Zanden, A. J.; Kerkhof, P. J. *Mol. Phys.* **1998**, *94* (3), 495−503.
(24) van de Ven-Lucassen, I. M.; Otten, A. M.; Vlugt, T. J.; Kerkhof, P. J. *Mol. Sim.* **1999**, *23*, 43−54.
(25) Wheeler, D. R.; Newman, J. *J. Phys. Chem. B* **2004**, *108*, 18362−18367.
(26) Onsager, L. *Phys. Rev.* **1931**, *37*, 405−426.
(27) Onsager, L. *Phys. Rev.* **1931**, *38*, 2265−2279.
(28) Kirkwood, J. G.; Buff, F. P. *J. Chem. Phys.* **1951**, *19* (6), 774−777.
(29) Chitra, R.; Smith, P. E. *J. Chem. Phys.* **2001**, *114* (1), 426−434.
(30) Zwanzig, R. *J. Chem. Phys.* **1964**, *40* (9), 2527−2533.
(31) Chandler, D. *Introduction to Modern Statistical Mechanics*; Oxford University Press: New York, 1987.
(32) Evans, D. J.; Morriss, G. P. *Statistical Mechanics of Nonequilibrium Liquids*; Academic Press: London, 1990.
(33) Hoheisel, C.; Vogelsang, R. *Comput. Phys. Rep.* **1988**, *8*, 1−70.
(34) Rowley, R. L. *Statistical Mechanics for Thermophysical Property Calculations*; Prentice-Hall: Englewood Cliffs, NJ, 1994.
(35) MacGowan, D.; Evans, D. J. *Phys. Rev. A* **1986**, *34* (3), 2133-2142.
(36) Rowley, R.; Stoker, J.; Giles, N. *Int. J. Thermophys.* **1991**, *12* (3), 501−513.
(37) Sarman, S.; Evans, D. J. *Phys. Rev. A* **1992**, *45* (4), 2370−2379.
(38) Maginn, E. J.; Bell, A. T.; Theodorou, D. N. *J. Phys. Chem.* **1993**, *97*, 4173−4181.
(39) Lee, J. *Physica A* **1997**, *243*, 229−242.
(40) Lee, J. *Physica A* **1997**, *247*, 140−152.
(41) van de Ven-Lucassen, I. M.; Vlugt, T. J.; van der Zanden, A.; Kerkhof, P. J. *Mol. Simul.* **1999**, *23*, 79−94.
(42) Müller-Plathe, F.; van Gunsteren, W. F. *J. Chem. Phys.* **1995**, *103* (11), 4745−4756.
(43) Chowdhuri, S.; Chandra, A. *J. Chem. Phys.* **2001**, *115* (8), 3732−3741.
(44) Tyrrell, H.; Harris, K. *Diffusion in Liquids*; Butterworths: London, 1984.
(45) McLennan, J. *Introduction to Nonequilibrium Statistical Mechanics*; Prentice Hall: Englewood Cliffs, NJ, 1989.
(46) Berne, B.; Harp, G. *Adv. Chem. Phys.* **1970**, *17*, 63−227.
(47) Hansen, J.-P.; McDonald, I. R. *Theory of Simple Liquids*; Academic Press: New York, 1986.
(48) Allen, M.; Tildesley, D. *Computer Simulation of Liquids*; Oxford Science: New York, 1989.
(49) Frenkel, D.; Smit, B. *Understanding Molecular Simulation*, 2nd ed.; Academic Press: New York, 2001.
(50) Mori, H. *Prog. Theor. Phys.* **1965**, *33*, 423.
(51) Evans, D. J.; Morriss, G. P. *Comput. Phys. Rep.* **1984**, *1*, 297−343.
(52) Morriss, G. P.; Evans, D. J. *Phys. Rev. A* **1987**, *35* (2), 792−797.
(53) Chapman, T. W. *The Transport Properties of Concentrated Electrolytic Solutions* Ph.D. Thesis, University of California, Berkeley, 1967.
(54) Wheeler, D. R.; Newman, J. *Chem. Phys. Lett.* **2002**, *366*, 537−543.
(55) Wheeler, D. R.; Rowley, R. L. *Mol. Phys.* **1998**, *94* (3), 555−564.
(56) Berendsen, H.; Grigera, J.; Straatsma, T. *J. Phys. Chem.* **1987**, *91*, 6269−6271.
(57) Guillot, B.; Guissani, Y. *J. Chem. Phys.* **2001**, *114* (15), 6720−6733.
(58) Lide, D. R., Ed. *CRC Handbook of Chemistry and Physics*, 73rd ed.; CRC Press: Boca Raton, FL, 1992.
(59) Koneshan, S.; Rasaiah, J. C.; Lynden-Bell, R.; Lee, S. *J. Phys. Chem. B* **1998**, *102*, 4193−4204.
(60) Koneshan, S.; Lynden-Bell, R.; Rasaiah, J. C. *J. Am. Chem. Soc.* **1998**, *120*, 12041−12050.
(61) Lybrand, T. P.; Kollman, P. A. *J. Chem. Phys.* **1985**, *83* (6), 2923−2933.
(62) Daivis, P. J.; Evans, D. J. *J. Chem. Phys.* **1994**, *100* (1), 541−547.
(63) Impey, R.; Madden, P.; McDonald, I. *J. Phys. Chem.* **1983**, *87*, 5071−5083.
(64) Ying, S.; Vattulainen, I.; Merikoski, J.; Hjelt, T.; Ala-Nissila, T. *Phys. Rev. B* **1998**, *58* (4), 2170−2178.
(65) Barthel, J. M.; Krienke, H.; Kunz, W. *Physical Chemistry of Electrolyte Solutions: Modern Aspects*; Springer: New York, 1998.
(66) Dufreche, J.-F.; Bernard, O.; Turq, P.; Mukherjee, A.; Bagchi, B. *Phys. Rev. Lett.* **2002**, *88* (9), 95902.
(67) Pitzer, K. S. *J. Am. Chem. Soc.* **1980**, *102*, 2902.
(68) Pitzer, K.; Simonson, J. *J. Phys. Chem.* **1986**, *90*, 3005.